Atomic-Scale Quantum Solvation Structure in Superfluid Helium-4 Clusters

Yongkyung Kwon
Department of Physics and Center for Advanced Materials and Devices, Konkuk University, Seoul 143-701, Korea

K. Birgitta Whaley
Department of Chemistry, University of California, Berkeley, California 94720
(Received 24 May 1999)

The local superfluid density around a molecule embedded in a ^4He_N cluster at low temperatures is analyzed using the path-integral Monte Carlo method. The molecular interaction induces a local nonsuperfluid component within a quantum solvation shell whose size is determined by the range of the molecule-helium interaction, and also introduces an anisotropic layering of the superfluid density around the molecule. We show that a local quantum hydrodynamic analysis is internally consistent for $N > 50$, and can be used to calculate effective rotational constants for molecular dopants in superfluid helium.

PACS numbers: 67.40.Hf, 36.40.Mr, 67.40.Yv

Clusters of ^{4}He constitute a finite-size quantum liquid which have recently been shown to provide an excellent environment for performing high resolution molecular and cluster spectroscopy [1]. The superfluid character of these clusters was recently demonstrated to be crucial in allowing the observation of fine structure due to molecular rotations, which is absent in normal liquids [2]. Conversely, dopant spectroscopy in ^4He_N offers an attractive new route to the study of quantum solvation phenomena in superfluids. A wide range of species can now be doped into a helium cluster by pickup techniques [1,3] and probed spectroscopically within the flight time of a cluster beam, effectively circumventing the problems associated with achieving equilibrium solvation in bulk helium. In this paper, we analyze the helium response to a molecular probe in ^4He_N, with a full microscopic determination of the atomic scale influence of the molecule on the local superfluid and normal fluid densities. This provides the first characterization of the decay (commonly known as the "healing") of the superfluid component near a microscopic boundary. We examine the temperature dependence of the nonsuperfluid component, and conclude that this consists of both a thermal contribution and a residual molecular-interaction-induced contribution, the latter of which is determined by the strength of the molecule-helium interaction potential. Analysis of the energetics, together with the superfluid response, provides a consistent quantum hydrodynamic picture for clusters of size $N > 50$, which can be used to calculate effective molecular rotational constants for impurity molecules in superfluid helium.

The thermodynamic properties of an N-particle helium-4 system at low temperatures T are determined by the Bose-symmetrized density matrix,

$$\rho_B(R, R'; \beta) = \frac{1}{N!} \sum_{\mathcal{P}} \rho(R, \mathcal{P}R'; \beta), \qquad (1)$$

where $\mathcal{P}$ denotes a permutation among helium atoms. In the discrete path-integral representation, $\rho(R, \mathcal{P}R'; \beta)$ is written as

$$\rho(R, \mathcal{P}R'; \beta) = \int \cdots \int dR_1 dR_2 \ldots dR_{M-1}\, \rho(R, R_1; \tau) \times \rho(R_1, R_2; \tau) \ldots \rho(R_{M-1}, \mathcal{P}R'; \tau), \qquad (2)$$

where $\beta = 1/k_B T$, $\tau = \beta/M$ is the imaginary time step, and R is the $3N$-dimensional position vector. The sum over permutations in Eq. (1) combined with the integration in Eq. (2) can be evaluated in path-integral Monte Carlo (PIMC) by a stochastic sampling of the discrete paths $\{R, R_1, R_2, \ldots, R_{M-1}, \mathcal{P}R'\}$, which is done here with the multilevel Metropolis algorithm of Ceperley and Pollock [4]. This approach is a computational realization of Feynman's idea of mapping path integrals of a quantum system onto interacting classical *polymers*. We present explicit calculations for SF_6 in ^4He_N, using the isotropic He-He [5] and anisotropic He-SF_6 [6] pair potentials. For pure helium-4 systems, accurate PIMC results can be achieved with the pair-product form of the exact two-body density matrices at $\tau^{-1} \geq 40$ K [7]. A heavy dopant species such as SF_6 in ^4He_N can be treated as providing an anisotropic external field for the helium atoms, which is incorporated here with the *primitive* approximation, requiring somewhat higher starting temperatures, i.e., smaller imaginary time steps. We find that converged anisotropic density profiles for the ^{4}He component are obtained using $\tau^{-1} \geq 80$ K. As in the $T = 0$ calculation of Ref. [8], our PIMC density profiles show a shell structure, with the first shell peaked at 4–5 Å from SF_6 which is located at the center of the cluster. The molecular rotational degrees of freedom are not included, so there is no explicit coupling of molecular rotational motion to the helium. Consequences of this restriction are examined below.

The *total* superfluid fraction can be evaluated within linear response theory from PIMC, using the projected

 0031-9007/99/83(20)/4108(4)$15.00

area estimator $\rho_s^{(A)}$ [7,9]. This reflects the appearance of superfluidity whenever the size of cross-linked polymers, formed by a product of cyclic permutation moves, becomes comparable to the dimension of the system. While this global estimator goes to the thermodynamic limit for large enough clusters, it does not, however, allow *local* structure in the superfluid density around the impurity to be investigated. To obtain a local estimator capable of analyzing anisotropic inhomogeneous structure, $\rho_s(\vec{r})$, we employ the density distribution of helium atoms participating in exchanges which are long compared to the system size. In pure ^4He_N, as in the bulk, the probability for such long paths increases dramatically as the cluster attains an appreciable global superfluid fraction [9]. Figure 1 shows the decomposition of the full radial density distribution for $^4He_N SF_6$ with $N = 64$ into contributions from exchange paths of length p, at $T = 0.625$ K. There is a clear distinction between the contribution of exchanges involving less than six atoms, and that from longer exchanges.

We define then a local superfluidity around a dopant molecule by summing all local exchange path densities longer than a minimum P:

$$\rho_s^{(P)}(\vec{r}) = \sum_{p' \geq P}^{N} \rho_{p'}(\vec{r}) \,. \tag{3}$$

For clusters with $N > 50$, we find that $P = 6$ yields a robust estimator of $\rho_s(\vec{r})$ in the local molecular environment, because most polymers sampled at low temperatures involve either a single atom (no exchange) or a very large number of atoms (long exchange). For smaller clusters, the short exchange paths are sampled more frequently so that it is not possible to make a clear distinction between the normal and the superfluid component from the length of the exchange paths. This is quantified in Table I by the first shell superfluid fraction estimator $\bar{\rho}_s^{(P)}$, obtained by integrating $\rho_s^{(P)}(\vec{r})$ over the first shell and normalizing by the corresponding total density. Also shown is a global superfluid fraction estimator $\rho_s^{(P)}$ obtained by integrating Eq. (3) over the entire cluster. Both $\bar{\rho}_s^{(P)}$ and $\rho_s^{(P)}$ show a decreasing dependence on P as the cluster size N increases, with the first shell superfluid estimator $\bar{\rho}_s^{(P)}$ appearing robust to the cutoff P for $N > 50$ ($\bar{\Delta}_s \leq 0.1$). This implies that $N \sim 50$ provides a lower limit for application of a quantum hydrodynamic analysis to the *local* helium environment in the doped cluster. We note that this minimum size is considerably larger than the size of the first solvation layer, $N \sim 22$–23 atoms [8]. Over this size range, the integrated superfluid fraction $\rho_s^{(P)}$ is somewhat smaller than the projected area estimator $\rho_s^{(A)}$ (by $\sim$0.06 for $N = 128$), but approaches this as N increases. The increase of $\rho_s^{(P)}$ with cluster size N (Table I) reflects the decreasing relative effect of the impurity in disturbing the long exchange paths characterizing the superfluid state. Based on this analysis of the length of the exchange paths, we employ $\rho_s(\vec{r}) \equiv \rho_s^{(P)}(\vec{r})$ with $P = 6$ as the fundamental local superfluid estimator for an impurity-doped cluster.

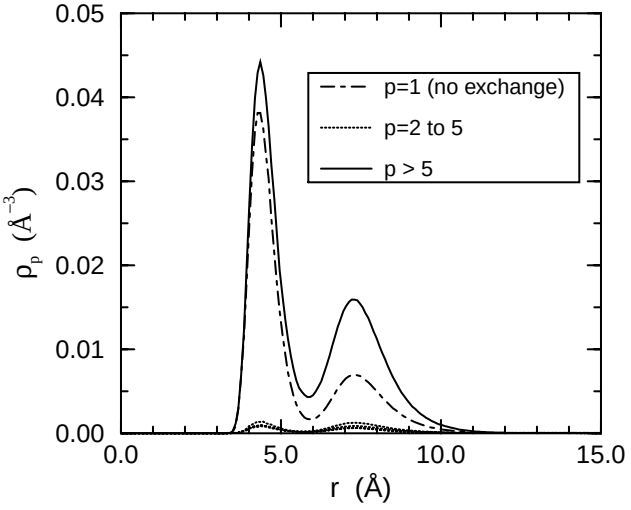

FIG. 1. Radial density contributions $\rho_p(r)$ from helium exchange paths of variable length p, for $^4He_N SF_6$ with $N = 64$. r is measured from the SF_6 center of mass.

Figure 2(a) shows the superfluid radial density distribution, $\rho_s(r)$, and 2(b) shows the corresponding ratios of superfluid to total density (i.e., the local superfluid fraction) for three different size clusters, $N = 50, 64$, and 128, at $T = 0.625$ K. The superfluid density shows a two layer structure around the molecule similar to that previously established for the total density [8]. This reflects the role of the repulsive component of the He-He interaction in providing some degree of hard core packing, although these quantum solvation layers cannot be characterized as solid. In the first solvation shell, $\rho_s(r)$ becomes independent of N for $N > 50$. This stability is consistent with the stability of the total density in the first shell when additional helium is added outside this [8]. For $N > 50$, as shown in Table I and Fig. 2(b), the superfluid fraction in the first solvation shell is about 50%. Beyond the first shell, however, it increases from 50% for $N = 50$, to $\sim$80% for $N = 128$, approaching the global fractions in

TABLE I. First shell integrated superfluid fraction, $\bar{\rho}_s^{(P)}$, and global superfluid fraction, $\rho_s^{(P)}$, in $^4He_N SF_6$ at $T = 0.625$ K. The robustness of $\bar{\rho}_s^{(P)}$ and $\rho_s^{(P)}$ with respect to P is measured by $\bar{\Delta}_s$ and Δ_s, respectively, where $\Delta \equiv (\rho^{(2)} - \rho^{(6)})/\rho^{(6)}$.

	First shell			Global		
N	$\bar{\rho}_s^{(2)}$	$\bar{\rho}_s^{(6)}$	$\bar{\Delta}_s$	$\rho_s^{(2)}$	$\rho_s^{(6)}$	Δ_s
12	0.45	0.16	1.81	0.45	0.16	1.81
23	0.58	0.42	0.38	0.58	0.42	0.38
39	0.64	0.52	0.23	0.65	0.52	0.25
50	0.64	0.55	0.16	0.66	0.54	0.22
64	0.55	0.51	0.08	0.68	0.58	0.17
128	0.64	0.58	0.10	0.78	0.68	0.14

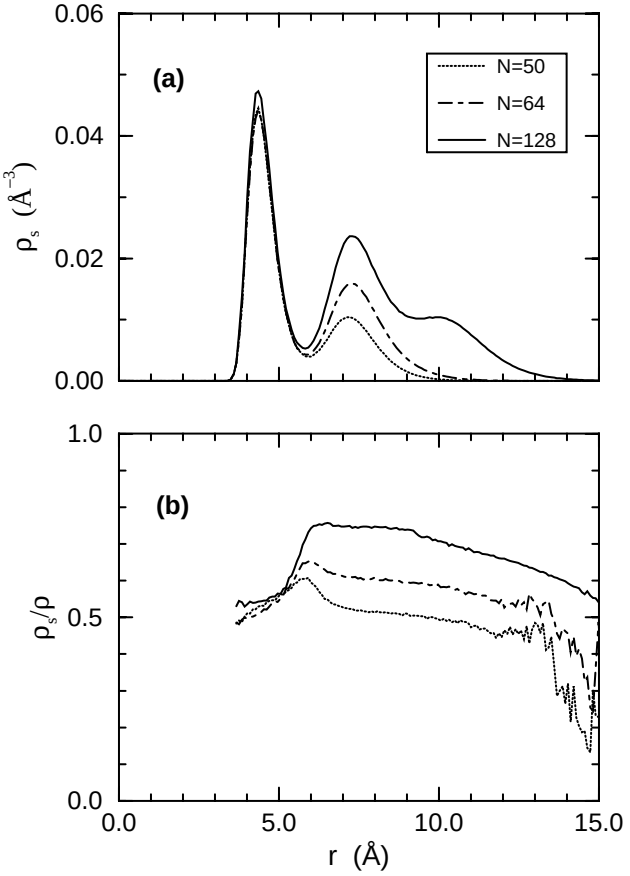

FIG. 2. Radial distributions of (a) superfluid density $\rho_s(r)$, and (b) the local superfluid fraction $\rho_s(r)/\rho(r)$, for $^4He_N SF_6$ with $N = 50, 64$, and 128, at $T = 0.625$ K. r is measured from the molecule center of mass.

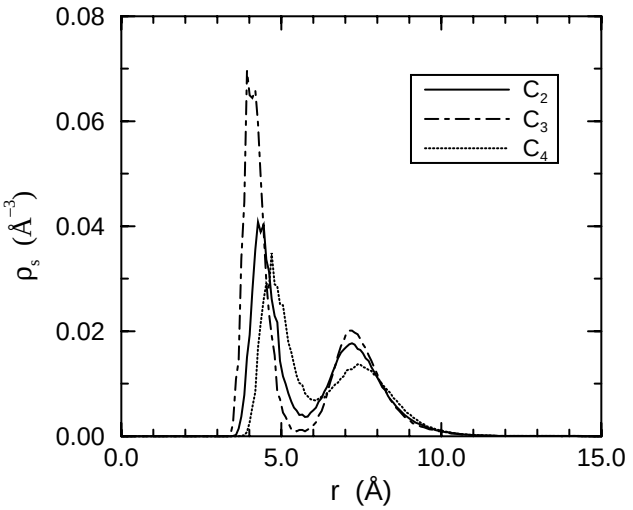

FIG. 3. Superfluid density distributions $\rho_s(\vec{r})$ along the three different SF_6 molecular symmetry axes, C_3, C_2, and C_4, in $^4He_{64}SF_6$ at $T = 0.625$ K. r is measured from the molecule center of mass.

pure ^4He_N clusters of these sizes [9]. This has two important implications. First, the PIMC value for the superfluid fraction in the first solvation shell found here for $N \leq 128$ will be valid also for larger clusters. Second, in the much larger clusters probed experimentally ($N \geq 1000$ [1,10]) the helium liquid outside the first shell can be assumed to be entirely in the superfluid state at these temperatures. We also find that, like the total density [8], the local superfluid density is strongly anisotropic. This is illustrated in Fig. 3 for $N = 64$, with profiles of $\rho_s(\vec{r})$ along the three symmetry axes of the SF_6 impurity.

The gross structure of this local superfluid density around the impurity molecule differs markedly from the smooth behavior predicted by the standard Ginzburg-Pitaevskii theory of healing [11]. The atomic scale structure seen here is a direct consequence of the greater strength of the molecule-helium interaction, relative to the He-He interaction. Analysis of these local densities over the temperature range $T = 0.3125-0.75$ K implies that the nonsuperfluid density contains both a thermal component and a molecular-interaction-induced component which is only weakly dependent on temperature. The latter is specific to the molecular dopant, exists on the length scale characteristic of the molecule-helium interaction, shows structure related to the symmetry of this, and will persist down to $T = 0$. A zero-temperature nonsuperfluid fraction around an impurity is in general accord with behavior at bulk interfaces inferred from third sound experiments [12–14] and also with quantum phase transition theory predictions for disordered interfaces [15,16]. However, this is the first analysis showing *atomic scale structure* in the residual nonsuperfluid fraction in a superfluid helium-4 system. The underlying origin of this atomic scale structure in the anisotropic molecule-helium interaction emphasizes the role of the molecule as an impurity which locally interrupts the phase coherence of the superfluid, analogous to the effect of magnetic impurities in superconductors [17] and aerogels in helium-3 [18]. We note that the molecular-interaction-induced nonsuperfluid component implies that the *global* superfluid fraction for a small cluster can be less than unity at $T = 0$.

Analysis of the PIMC energetics shows only a very small decrease in the total energy [$\Delta E \sim 0.06(3)$ K per He atom] as the temperature is lowered over the range $T = 0.75-0.31$ K. This is a consequence of the fact that these temperatures are well below the broadened superfluid transition in finite ^4He_N for these sizes [9]. Although the molecular rotational degrees of freedom are not explicitly included in these calculations, we can conclude that the nonsuperfluid density in the first solvation shell will adiabatically follow the molecular rotation, because the potential energy decrease resulting from the strong angular modulation of the potential [6] is far larger than a semiclassical estimate of the nonsuperfluid rotational kinetic energy. Zero-temperature diffusion Monte Carlo calculations incorporating molecular rotational degrees of freedom yield density profiles supporting the notion of adiabatic following of some fraction of the

helium density around the SF_6 [19,20]. This leads to a two-fluid analysis for the rotational dynamics of an impurity molecule in a ^4He_N cluster in the hydrodynamic regime ($N > 50$). First, the adiabatic response of the nonsuperfluid component results in the effective moment of inertia $I = I_0 + \Delta I_n$, with

$$\Delta I_n = m_4 \int_0^{R_c} \int_0^{\pi} \int_0^{2\pi} \rho_n(r, \theta, \phi) r^4 \sin^3\theta \, dr \, d\theta \, d\phi \,, \tag{4}$$

where R_c is the range of the adiabatic coupling to the normal fraction, I_0 is the gas-phase value, and m_4 is the ^{4}He atomic mass. R_c is determined by the range of the local *anisotropic* nonsuperfluid density formed as a result of the strong molecule-helium interaction, $\rho_n(\vec{r}) = \rho(\vec{r}) - \rho_s(\vec{r})$. For very large clusters ($N \geq 1000$) this can be approximated by the width of the first solvation layer, since the superfluid fraction goes to unity in the outer region (see above). Second, superfluid kinetic energy generated by the molecular boundary motion increases the energy required for rotational excitation of the molecule in the cluster. Hydrodynamic calculations within a continuum model indicate that this superfluid contribution is very small for SF_6 [20]. In this quantum hydrodynamic picture, the dual effect of decoupling of local superfluid density from the molecular rotation, and adiabatically induced rigid coupling of the molecular motion to the local nonsuperfluid density, will therefore give rise to a spectroscopic signature of apparent free molecular rotation with increased moment of inertia (reduced rotational constants). This two-fluid analysis has been used, together with the PIMC local nonsuperfluid densities, to calculate the SF_6 effective rotational constant in ^4He_N in the hydrodynamic regime, $N > 50$ [20]. A value of 1.02 ± 0.03 GHz is obtained for $T = 0.3$–0.4 K, in excellent agreement with experimental values derived from infrared spectra measured in larger clusters [10], providing additional confirmation that the contribution from superfluid backflow is indeed negligible.

The adiabatic following of the local nonsuperfluid density which gives rise to reduced rotational constants is an intrinsic feature of an *anisotropic* molecular environment. It is predicted to be present also at zero temperature, unlike the thermally generated normal fluid density which provides drag on macroscopic rotating objects in the classic Andronikashvili analysis [21]. Another significant distinction from the latter is that rigid coupling of the nonsuperfluid density deriving from adiabatic following preserves the rotational coherence of a molecule, giving rise to a discrete spectrum, whereas for a macroscopic object a *classical* measurement of the moment of inertia is made. An interesting question for further study is the symmetry of the local nonsuperfluid density, the directionality of its adiabatic following, and how this is related to the molecular symmetry and to modifications of this induced by complexation [22]. Addition of a second impurity atom or molecule can lower the symmetry of the molecular boundary seen by the helium, give rise to a nonsuperfluid distribution unrelated to the original molecular symmetry, and introduce adiabatic following in new directions. This can modify the symmetry of the spectroscopically measured rotational constants. Complexes assembled in superfluid helium clusters therefore present new challenges for analysis, as well as new opportunities for probing microscopic structure of superfluids near interfaces.

This work has been supported by the Korea Ministry of Education under Grant No. BSRI-96-2456, and by the Chemistry Division of the National Science Foundation under Grant No. CHE-9616615.

[1] J. P. Toennies and A. F. Vilesov, Annu. Rev. Phys. Chem. **49**, 1 (1998).
[2] S. Grebenev, J. P. Toennies, and A. F. Vilesov, Science **279**, 2083 (1998).
[3] S. Goyal, D. L. Schutt, and G. Scoles, J. Phys. Chem. **97**, 2236 (1993).
[4] D. M. Ceperley and E. L. Pollock, Phys. Rev. Lett. **56**, 351 (1986).
[5] R. A. Aziz, F. R. W. McCourt, and C. C. K. Wong, Mol. Phys. **61**, 1487 (1987).
[6] R. T. Pack *et al.*, Chem. Phys. **80**, 4940 (1984).
[7] D. M. Ceperley, Rev. Mod. Phys. **67**, 279 (1995).
[8] R. N. Barnett and K. B. Whaley, J. Chem. Phys. **99**, 9730 (1993).
[9] P. Sindzingre, M. L. Klein, and D. M. Ceperley, Phys. Rev. Lett. **63**, 1601 (1989).
[10] M. Hartmann *et al.*, Phys. Rev. Lett. **75**, 1566 (1995).
[11] V. L. Ginzburg and L. P. Pitaevskii, Sov. Phys. JETP **7**, 858 (1958).
[12] P. J. Shirron and J. M. Mochel, Phys. Rev. Lett. **67**, 1118 (1991).
[13] P. W. Adams and V. Pant, Phys. Rev. Lett. **68**, 2350 (1992).
[14] G. Zimmerli, G. Mistura, and M. H. W. Chan, Phys. Rev. Lett. **68**, 60 (1992).
[15] M. P. Fisher *et al.*, Phys. Rev. B **40**, 546 (1989).
[16] P. A. Crowell, F. W. Van Keuls, and J. D. Reppy, Phys. Rev. B **55**, 12 620 (1997).
[17] A. Yazdani *et al.*, Science **275**, 1767 (1997).
[18] K. Matsumoto *et al.*, Phys. Rev. Lett. **79**, 253 (1997).
[19] E. Lee, D. Farrelly, and K. B. Whaley, Phys. Rev. Lett. **83**, 3812 (1999).
[20] Y. Kwon *et al.* (to be published).
[21] E. L. Andronikashvili, J. Phys. (Moscow) **10**, 201 (1946).
[22] M. Hartmann *et al.*, Science **272**, 1631 (1996).